Remote Sensing of Environment 115 (2011) 3424–3435

Contents lists available at SciVerse ScienceDirect

Remote Sensing of Environment

journal homepage: www.elsevier.com/locate/rse

Predicting gross primary production from the enhanced vegetation index and photosynthetically active radiation: Evaluation and calibration

Chaoyang Wu [a,b,*], Jing M. Chen [b], Ni Huang [a]

[a] The State Key Laboratory of Remote Sensing Science, Institute of Remote Sensing Applications, Chinese Academy of Sciences, Beijing 100101, China
[b] Department of Geography, University of Toronto, 100 St. George St., Room 5047, Toronto, ON, Canada M5S 3G3

ARTICLE INFO

Article history:
Received 24 May 2011
Received in revised form 10 August 2011
Accepted 13 August 2011
Available online 13 September 2011

Keywords:
Remote sensing
Gross primary production (GPP)
MODIS
Enhanced vegetation index (EVI)

ABSTRACT

The approach of using primarily satellite observations to estimate ecosystem gross primary production (GPP) without resorting to interpolation of many surface observations has recently shown promising results. Previous work has shown that the remote sensing based greenness and radiation (GR) model can give accurate GPP estimates in crops. However, the feasibility of its application and the model calibration to other ecosystems remain unknown. With the enhanced vegetation index (EVI) derived from the Moderate Resolution Imaging Spectroradiometer (MODIS) images and the surface based estimates of photosynthetically active radiation (PAR), we provide an analysis of the GR model for estimating monthly GPP using flux measurements at fifteen sites, representing a wide range of ecosystems with various canopy structures and climate characteristics. Results demonstrate that the GR model can provide better estimates of GPP than that of the temperature and greenness (TG) model for the overall data classified as non-forest (NF), deciduous forest (DF) and evergreen forest (EF) sites. Calibration of the GR model is also conducted and has shown reasonable results for all sites with a root mean square error of 47.18 g C/m^2/month. Different coefficients acquired for the three plant functional types indicate that there are shifts of importance among various factors that determine the monthly vegetation GPP. The analysis firstly shows the potential use of the GR model in estimating GPP across biomes while it also points to the needs of further considerations in future operational applications.

1. Introduction

Terrestrial ecosystems play important roles in the carbon sequestration and the global estimate of the carbon dioxide (CO_2) fixed by plants as organic compounds through photosynthesis of around 123 ± 8 Pg C per year (Beer et al., 2010). This flux is also known as the gross primary production (GPP) and is an important component for the carbon balance between the biosphere and the atmosphere (Zhao & Running, 2010). However, substantial variations of GPP are observed among different models and ecoregions both at plant and stand levels and these discrepancies prevent the full understanding of global carbon cycle. For example, the uncertainty within the most comprehensive GPP estimates of Beer et al. (2010) at present is roughly four times the annual CO_2 emissions from fossil-fuel burning (Reich, 2010). Therefore, improvements on the accuracy of GPP estimation are needed in the context of future climate change.

Satellite remote sensing provides a real opportunity to robustly estimate ecosystem GPP globally and therefore it helps both in developing and testing of these new models. A number of remote sensing based GPP models have been proposed, including the Moderate Resolution Imaging Spectroradiometer (MODIS) product termed MOD17 (Zhao et al., 2006), the Vegetation Photosynthesis Model (VPM, Xiao et al., 2004), and the Physiological Principles for Predicting Growth (3-PG, Coops et al., 2005). While models driven by a large number of input parameters can give good estimates of GPP, the demand of these variables at required temporal and spatial resolutions is often a bottleneck for the global applications of these models.

Therefore, a focus on the development of new GPP models is the potential of independence on climate variables or ground observations. For example, Sims et al. (2008) introduce a new model using the MODIS enhanced vegetation index (EVI, Huete et al., 2002) and land surface temperature (LST, Wan, 2008) products, termed as the greenness and temperature (TG) model. Similar attempts are also shown with the chlorophyll content model (Gitelson et al., 2006), in which the chlorophyll vegetation index and photosynthetically active radiation (PAR) are utilized to estimate GPP in crops. However, evaluation of these models has been limited in scope which reduces their potential for global applications (Wu et al., 2010). For example, the chlorophyll content model, referred as greenness and radiation (GR)

* Corresponding author at: Department of Geography, University of Toronto, 100 St. George St., Room 5047, Toronto, ON, Canada M5S 3G3. Tel.: +1 647 524 0310.
E-mail address: hefery@163.com (C. Wu).

0034-4257/$ – see front matter © 2011 Elsevier Inc. All rights reserved.
doi:10.1016/j.rse.2011.08.006

model hereafter, has only been tested in crops and the model calibration in other ecosystems is still unknown (Peng et al., 2011).

In this study, we report an evaluation of the GR model for interpreting GPP using multiple sites in different ecoregions with diverse canopy structures and climate characteristics. The TG model is also included for comparison analysis since a close relationship exists between these two models. The objectives of the present study are 1) to give a full evaluation of the GR model for estimating monthly GPP across a wide range of ecosystems of different plant functional types, 2) to show a comparison between the TG and the GR models in GPP estimation, and 3) to calibrate the GR model for GPP estimation for different plant functional types. These analyses will be useful for the future application of these models to better quantify CO_2 flux.

2. Materials and methods

2.1. Study sites

By knowing a single study site and vegetation type, we cannot represent the general response of models in different ecosystems. As shown in Fig. 1, 15 flux sites are selected in this study and these sites can be classified into three different plant functional types, including the non-forest sites (NF, 5 sites), the deciduous forest sites (DF, 5 sites) and the evergreen forest sites (EF, 5 sites). Detailed descriptions for each site are shown in Table 1.

2.2. Flux measurements

Flux data for CA-AB are downloaded from the Fluxnet Canada Data Information System (http://www.fluxnet-canada.ca) while data from the other AmeriFlux sites are acquired from http://public.ornl.gov/ameriflux/dataproducts.shtml. For CA-AB site, a standard procedure is used to estimate annual net ecosystem production (NEP) and to partition NEP into components of GPP and ecosystem respiration (Re) from gap-filled half-hourly measurements (Barr et al., 2004). For AmeriFlux sites, level-4 monthly products are used to acquire the monthly GPP, air temperature (T_a) and radiation observations. These data are gap-filled and GPP is estimated with the Artificial Neural Network (ANN) method (Papale & Valentini, 2003) and/or the Marginal Distribution Sampling (MDS) method (Reichstein et al., 2005). Site level PAR observations are acquired by using the in situ meteorological measurements.

For all sites, months with estimated GPP or the mean monthly T_a below zero are not used. Months from May to October for US-VAR and US-TON, sites that experience a Mediterranean climate with wet, mild winters and dry, hot summers, are also excluded in this analysis (Ma et al., 2007; Ryu et al., 2008).

2.3. MODIS product

The Terra MODIS atmospherically-corrected surface reflectance products, MOD09A1 (Justice et al., 2002) are acquired for each site

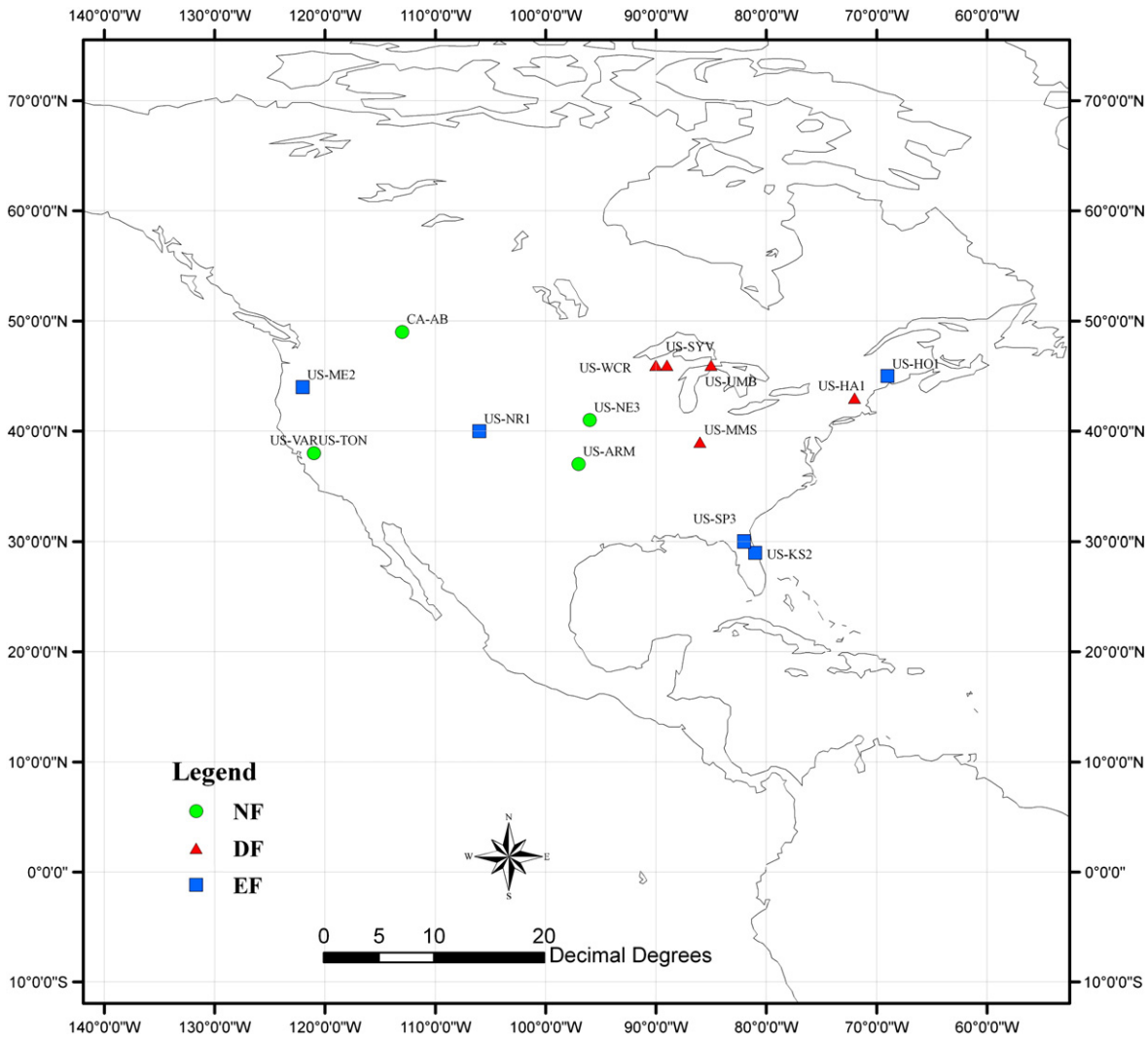

Fig. 1. Spatial distribution of the 15 sites in this study, the NF, DF and EF represent non-forests, deciduous forests and evergreen forests, respectively.

Table 1
Descriptions of flux sites in this study.

Sites		Land cover	Latitude and longitude	GPP_ave (g C/m^2/month)	Data range	References
Non-forest sites (NF)	CA-AB	Grassland	49.4300 −112.5600	137.88	2002–2005	Flanagan and Johnson (2005)
	US-VAR	Grassland	38.4133 −120.9507	108.39	2003–2006	Ryu et al. (2008)
	US-TON	Woody savannas	38.4316 −120.9660	21.82	2003–2007	Ma et al. (2007)
	US-NE3	Crop	41.1797 −96.4397	216.25	2002–2006	Suyker and Verma (2008)
	US-ARM	Crop	36.6058 −97.4888	68.25	2003–2006	Fischer et al. (2007)
Deciduous forest sites (DF)	US-HA1	Deciduous Board-leaf forest	42.5378 −72.1715	101.16	2002–2006	Urbanski et al. (2007)
	US-WCR	Deciduous Board-leaf forest	45.8059 −90.0799	172.76	2002–2006	Cook et al. (2004)
	US-UMB	Deciduous Board-leaf forest	45.5598 −84.7138	163.58	2002–2006	Curtis et al. (2002)
	US-MMS	Deciduous Board-leaf forest	39.3231 −86.4131	193.06	2002–2006	Dragoni et al. (2007)
	US-SYV	Deciduous Board-leaf forest	46.2420 −89.3477	161.47	2002–2006	Desai et al. (2008)
Evergreen forest sites (EF)	US-HO1	Evergreen Needle-leaf forest	45.2041 −68.7402	174.98	2002–2004	Hollinger et al. (2004)
	US-KS2	Evergreen Broad-leaf forest	28.6086 −80.6715	139.45	2004–2006	Powell et al. (2008)
	US-SP3	Evergreen Broad-leaf forest	29.7548 −82.1633	154.96	2002–2004	Dore et al. (2003)
	US-ME2	Evergreen needle-leaf forest	44.4523 −121.5574	143.37	2004–2007	Thomas et al. (2009)
	US-NR1	Evergreen needle-leaf forest	40.0329 −105.5460	103.37	2002–2007	Monson et al. (2005)

from the Oak Ridge National Laboratory's Distributed Active Archive Center (DAAC) website (http://www.modis.ornl.gov/modis/index.cfm). This eight-day reflectance is then used to calculate EVI. Cloud contaminated and high aerosol pixels are rejected by selecting the quality flag, which ensures the good quality of calculated EVI. Due to uncertainty in determination which pixel the footprint falls in, reflectance are extracted from 3×3 MODIS pixels (1.5 km×1.5 km) that centered on the flux tower. Three band reflectances (blue band: 459–479 nm; red band: 620–670 nm and the near-infrared band: 841–876 nm) are used to calculated the EVI using the equation below:

$$\mathrm{EVI} = 2.5\times\frac{R_{NIR}-R_{Red}}{1+R_{NIR}+6\times R_{Red}-7.5\times R_{\mathrm{Blue}}} \quad (1)$$

where R_x is the reflectance at the given wavelength (nm). Multiple observations of EVI during the same month are averaged to represent the mean monthly values.

2.4. GPP models

2.4.1. The TG model

The TG model is proposed by Sims et al. (2008) and estimates vegetation GPP using a combination of MODIS LST and EVI products. The most important merit of this model is the independence of climate variables. With close correlations between LST and environmental variables, such as PAR and vapor pressure deficit (VPD), the GPP can be estimated as a product of scaled canopy greenness (i.e., EVI) and scaled LST,

$$GPP = ScaledEVI\times ScaledLST. \quad (2)$$

Because GPP drops to zero at an average EVI around 0.1, the *Scaled*EVI is thus defined as,

$$Scaled\mathrm{EVI} = \mathrm{EVI} - 0.1. \quad (3)$$

Meanwhile, *ScaledLST* is proposed based on the determination of optimum temperature for GPP. As GPP generally increases to the maximum values at the LST around 30 °C, two linear equations are used to define the *ScaledLST*,

$$ScaledLST = \min\left[\left(\frac{LST}{30}\right),(2.5-0.05\times LST)\right]. \quad (4)$$

However, incorporation of MODIS LST can lead to error because satellite sensors measure a signal that is a combination of the radiant temperature of the land surface and the intervening atmosphere (Goetz et al., 2000). Therefore, we use a revised simple form of the original TG by using the air temperature (T_a, deg C) from the flux measurements. In order to keep consistent with the original TG model, an optimum temperature should be determined. As indicated by Sims et al. (2008) that MODIS LST tends to be higher than T_a at the upper end of the temperature range, this optimum temperature of T_a should be lower than 30 °C and therefore is set to 25 °C in this study, given the average difference of ~5 K in MODIS LST evaluations (Wan, 2008; Westermann et al., 2011). Therefore, the following equation is used for this revised TG model,

$$GPP = (\mathrm{EVI}-0.1)\times\min(T_a, 50-T_a). \quad (5)$$

2.4.2. The GR model

The GR model is first introduced by Gitelson et al. (2006) in both irrigated and rainfed maize. With observation of a close relationship between midday GPP and the total crop chlorophyll content, a new technique is proposed to estimate GPP by the product of total chlorophyll content and the incoming solar radiation. The GR model has shown high potential to predict GPP in crops (e.g., maize and soybean) with root mean square errors around 0.27 mg CO_2 m^{-2} s^{-1} (Gitelson et al., 2006; Peng et al., 2011). Recent validations of the model also show promising results in wheat (Wu et al., 2009).

Owing to the important role of total chlorophyll content, as well as its relationship with vegetation index, this method can be scaled up by using remotely sensed vegetation index as a proxy for the total chlorophyll content. Therefore, the model can be expressed by the following equation,

$$GPP = VI_{Chl} \times PAR \quad (6)$$

where the VI_{Chl} can be composed of the chlorophyll indices, such as the EVI that used in this study. The required incoming PAR data were acquired from the meteorological measurements at flux towers.

3. Results and discussion

3.1. Results of the TG and GR models

Results of both the TG and GR model are compared with the flux measured GPP for each site (Fig. 2a). For the five NF sites, the GR model generally shows better correlations with flux GPP than the TG model except for site NE3, at which the TG model gives the best estimates of GPP with a coefficient of determination R^2 of 0.91. For the other four NF sites, the GR model all shows higher potentials in GPP estimation with the highest R^2 equal to 0.94 at site TON. The most evident difference between the two model outputs is shown at site ARM, where low correlation has been found for the TG model ($R^2 = 0.27$) while the GR model can give moderate estimates of GPP with R^2 of 0.53. One shortcoming of the TG model is the limited ability in drought sites (Sims et al., 2008), and this is probably the reason for the poor performance at ARM site, which suffers from serious drought in this study. The underlying mechanism of this observation is that the drought will reduce the correlation between the temperature and PAR, which is the basis of the TG model (Sims et al., 2008). By using ground measured PAR directly, the GR model can still show moderate estimates of GPP. Both the TG and GR models show good estimates of GPP for the DF sites with all coefficients of determination of R^2 above 0.80 (Fig. 2b). These results indicate that both of the two models can have potentials in the estimation of GPP for ecosystems with relatively wide ranges of greenness. Substantial variations are observed for both models in the five EF sites (Fig. 2c). The TG model has shown the best result for HO1 with R^2 of 0.91 while only R^2 of 0.28 is observed for site SP3. A similar problem also appears with the GR model with R^2 fluctuates between the highest of 0.85 for HO1 and the lowest of 0.25 for NR1.

To give a further comparison between the two models, we group the 15 sites by their plant functional types (Fig. 3). Consistent results

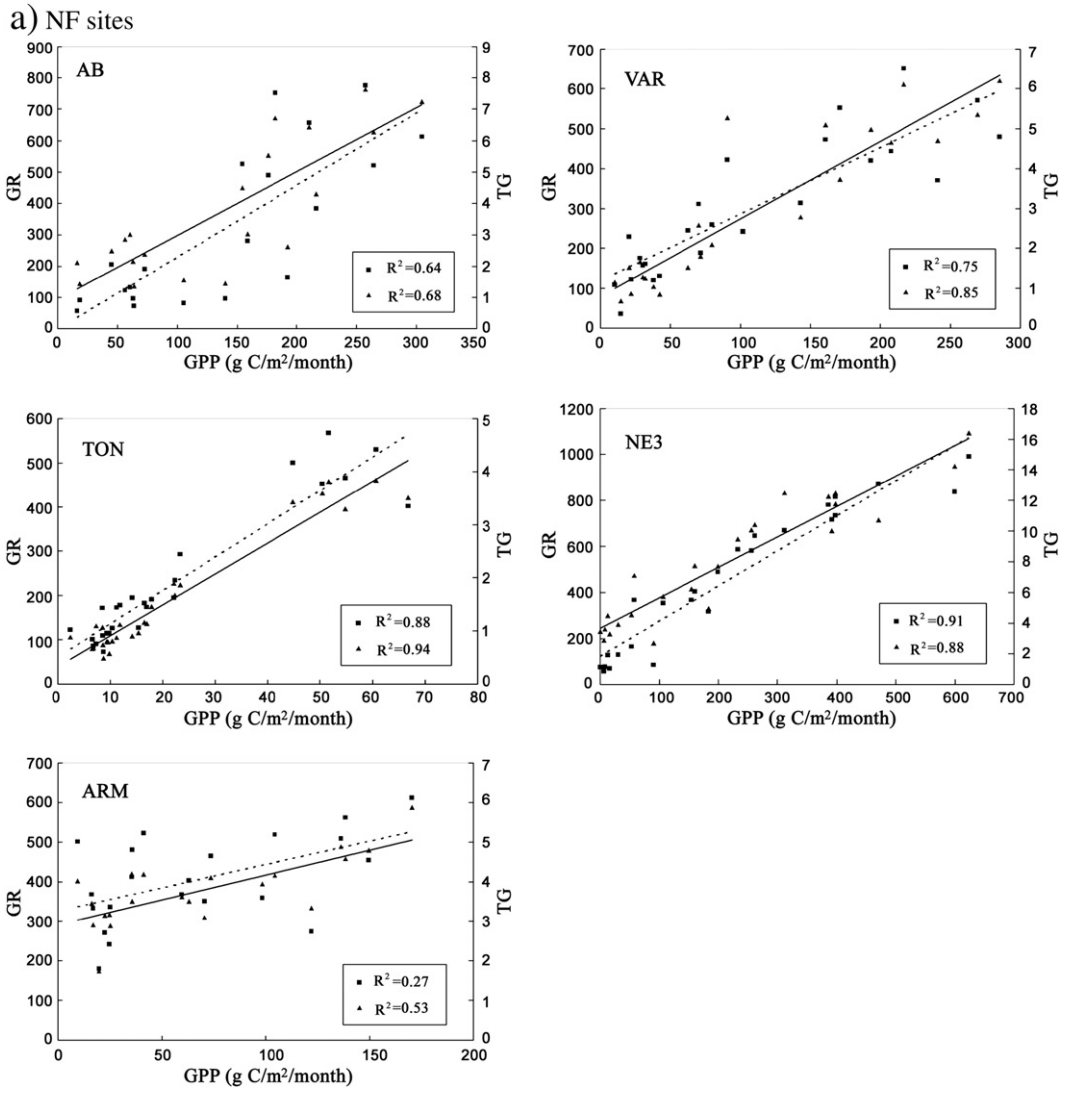

Fig. 2. Relationship between the flux measured GPP and results of TG, GR models for all sites divided into (a) non-forest sites, (b) deciduous forest sites and (c) evergreen forest sites. Rectangular and triangular points represent TG and GR model, respectively.

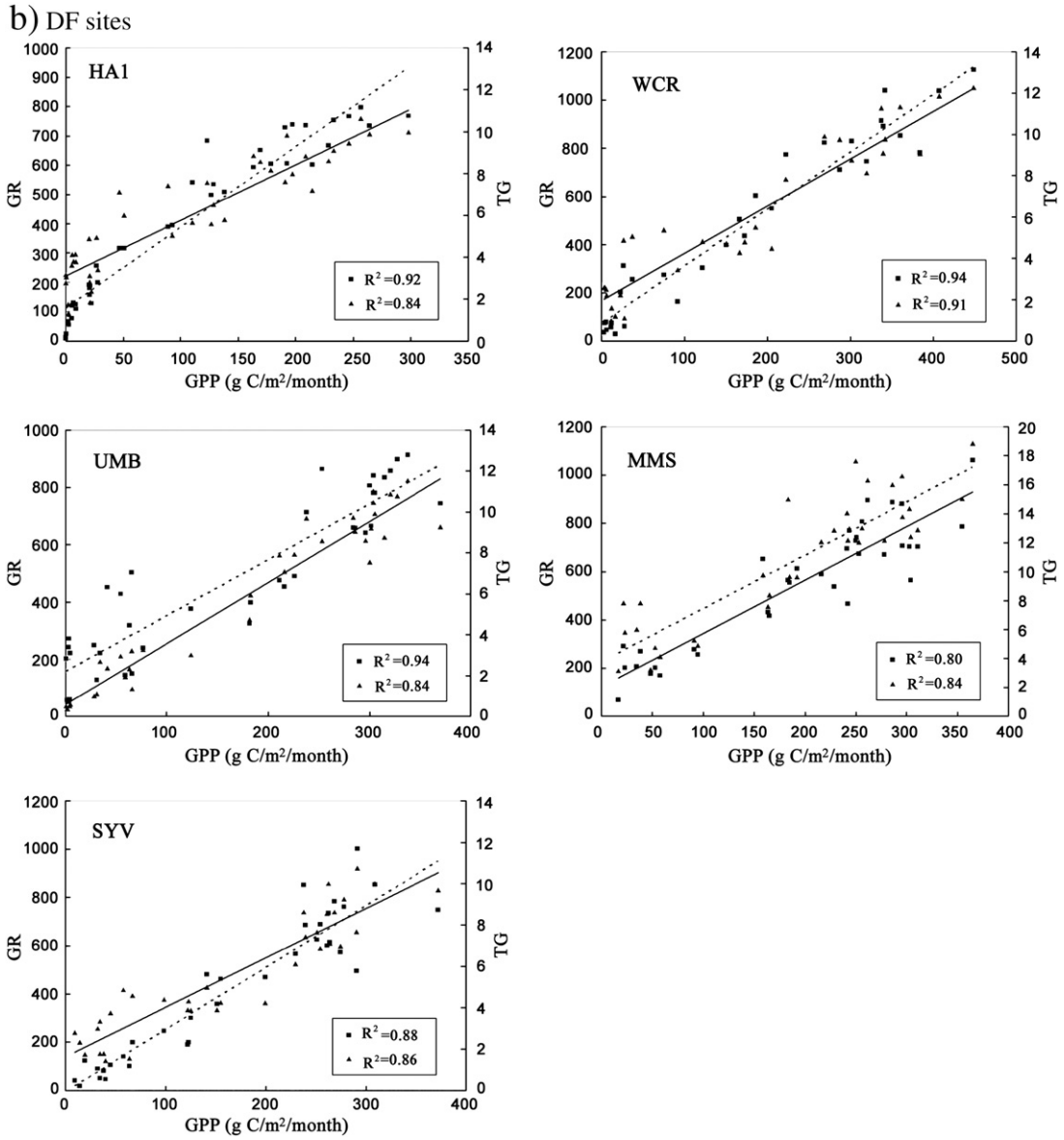

Fig. 2 (*continued*).

are observed for both models when considering different plant functional types. Best results are obtained for the DF sites, followed by the NF and EF sites. As both models partly capture the greenness of vegetation, a better response will be acquired for ecosystems with much wider dynamical ranges of EVI. Therefore, the DF sites which have the largest mean standard deviation in EVI (EVI_sd = 0.15) illustrate the best performances for both models. Similar explanations also make sense for the NF and EF sites with EVI_sd of 0.12 and 0.04, respectively. This probably is the reason for the best responses of both models at the HO1 site, which is sometimes classified as a mixed forest with the largest EVI_sd of 0.06 among the EF sites. When comparing between models, the GR model can give better results than the TG model with higher R^2 for all the three types and the overall dataset. In initial development of the TG model, the LST is incorporated because of two reasons. First, using LST will ensure no ground measurements for running the model. The second aspect is the correlation between LST and environmental variables, such as VPD and most importantly the PAR (Sims et al., 2008). It has been demonstrated that using T_a measured at the flux towers instead of MODIS LST can give better GPP estimates with the TG model as uncertainties in the satellite LST are excluded (Wu et al., 2010). However, here we find that for the EF sites, very low correlation is observed between T_a and PAR ($R^2 = 0.11$, Fig. 4), which probably is the main reason for the low R^2 ($R^2 = 0.31$) of the TG model for these EF sites (Fig. 4c). With PAR from ground measurements, the GR model can still show a potential in characterizing the GPP for EF sites with an overall R^2 of 0.47.

3.2. Calibration of the GR model

Model calibration is an important step for their operational applications and it is a challenge because the responses of biomes may differ under various vegetation structural and environmental conditions. Here we provide an analysis of GR model calibration in view of both greenness and environmental stresses and their relative importance.

With the correlation between GPP and the term EVI × PAR, the slope (S) of the regression for each plant functional types is obtained. For the NF sites, a perfect fit with R^2 of 0.99 ($p<0.001$) has been found between S and the difference between the maximum and the minimum monthly EVI (dEVI = EVI_max-EVI_min) during the experimental time range (Fig. 5a). Similar results for the DF and EF sites are shown in Fig. 5b

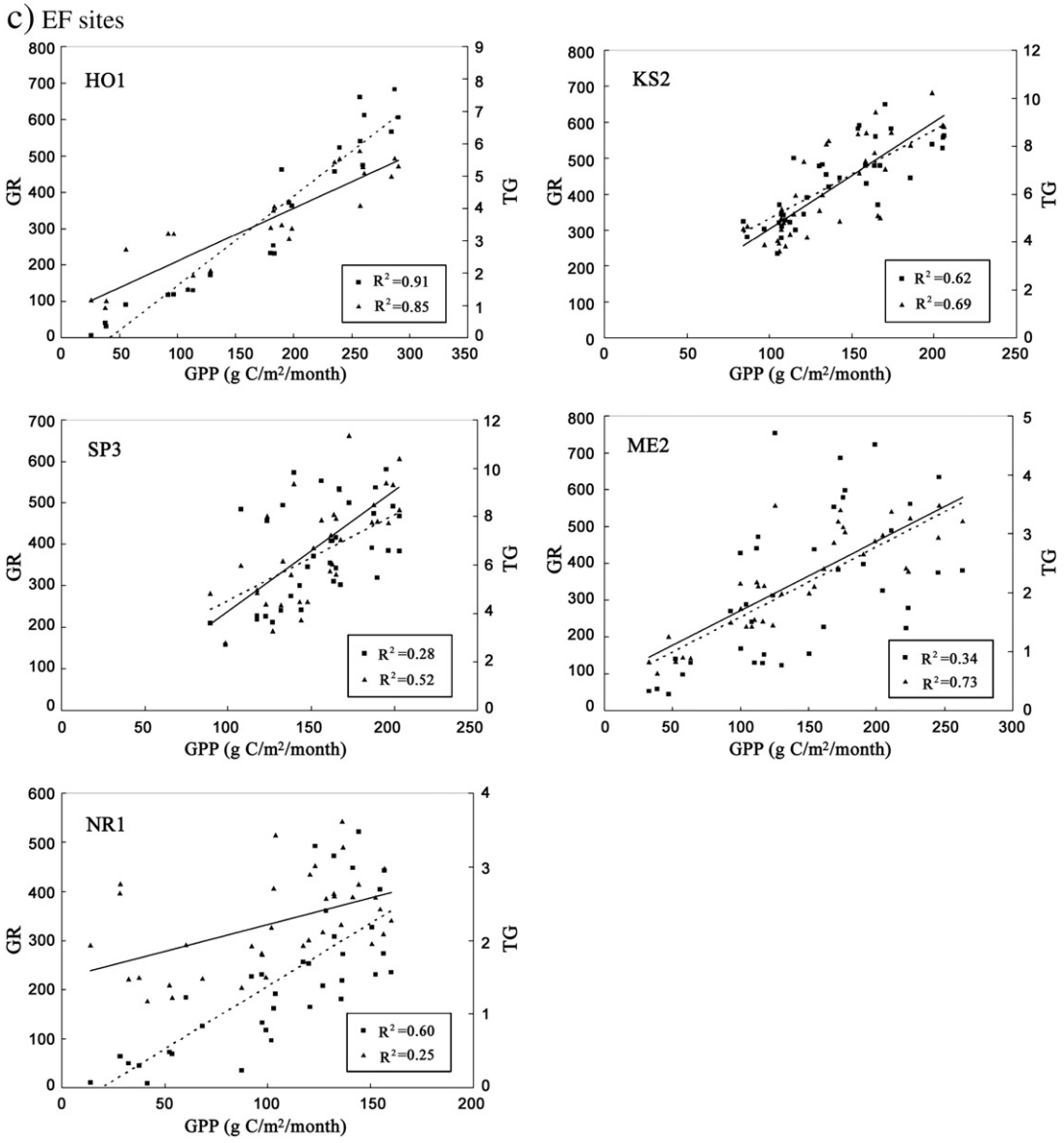

Fig. 2 (*continued*).

and c, respectively. We find that *S* for the DF sites is a function of the product of dEVI and the standard deviation of mean monthly temperature (T_sd) while *S* for the EF sites is directly correlated with the T_sd. Although there are only five sites for each type, all correlations are significant and the GR model can then be calibrated as:

$$\mathrm{GPP} = S\times(EVI\times PAR)$$
$$\text{and } S = \begin{cases} 1.17\times dEVI - 0.20, & \text{for the NF sites} \\ 0.24\times(dEVI\times T\_sd) - 0.31, & \text{for the DF sites} \\ 0.10\times T\_sd - 0.17, & \text{for the EF sites} \end{cases}. \quad (5)$$

The modeled monthly GPP (GPP_M) using these coefficients is then compared with flux measurements (GPP_F) for all sites (Fig. 6). For the NF sites, the GR model gives the best GPP estimates at site TON with a root mean square error (RMSE) of 5.07 g C/m^2/month. The largest RMSE is acquired for NE3 with a value of around 75 g C/m^2/month and the average RMSE for these NF sites is around 40 g C/m^2/month. Most of the DF sites show good estimates of GPP and the RMSE values generally fall between 40 and 60 g C/m^2/month. Due to much lower GPP values for the EF sites, lower RMSE values are also observed, which typically fluctuate between 30 and 45 g C/m^2/month. The RMSE for the overall data of all sites is 47.18 g C/m^2/month, which indicates that the accuracy of calibration is reasonable and these coefficients are of potential use in future applications (Fig. 7).

While the GR model shows reasonably good estimates of monthly GPP for most sites, there is a tendency of overestimation during the early part of the growing seasons. For example, for site TON, modeled monthly GPP was systematically higher than the flux measurements at GPP values larger than 30 g C/m^2/month. This tendency exists for all the other four NF sites when monthly GPP falls below 100 g C/m^2/month. All DF sites show similar situations, only differing in the peak values of this overestimation. The EF sites seem not affected as much by this overestimation compared to the NF and DF sites, although this limitation is shown for site NR1. We suggest that there are three reasons that can be referred to explain these overestimations. First is the uncertainty associated with the MODIS reflectance data that is used for the calculation of EVI. For both the NF and DF sites, the EVI shows relatively large dynamical ranges (e.g., mean EVI_max = 0.65 and mean EVI_min = 0.18 for sites in this study) and this could lead to large errors or uncertainty for the low EVI values during the early growth stages. This is because of the

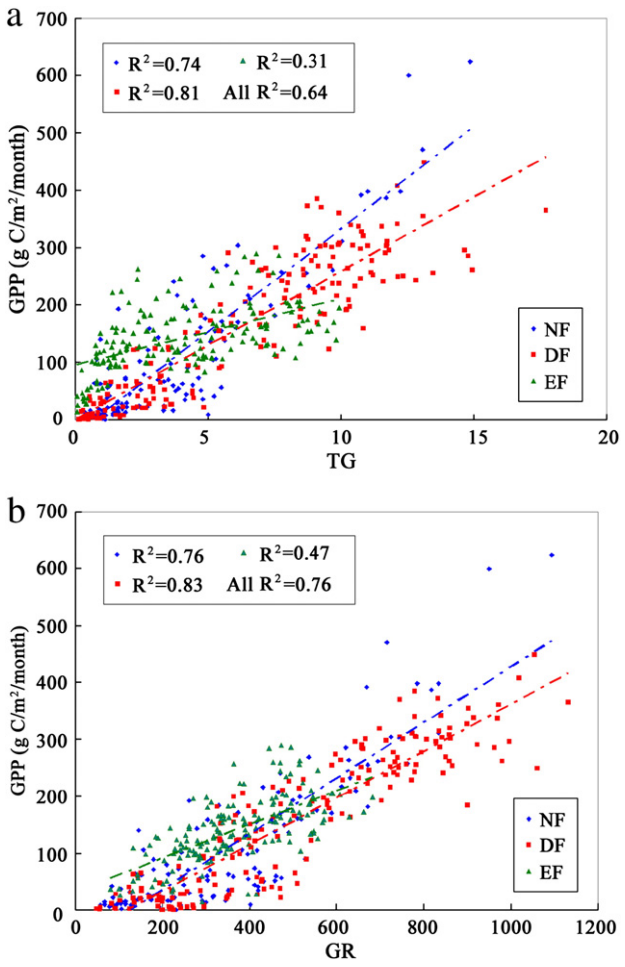

Fig. 3. Comparison between (a) TG and (b) GR results for different plant functional types (NF, DF and EF represent non-forests, deciduous forests and evergreen forests, respectively).

relatively large effects from the background information (e.g., soil) for the sparse canopies. This overestimation could be even larger when considering the cloud contaminations. A second explanation is the biochemical functions of leaves for photosynthesis. During the early growing season, there is a possibility that parts of the green leaves

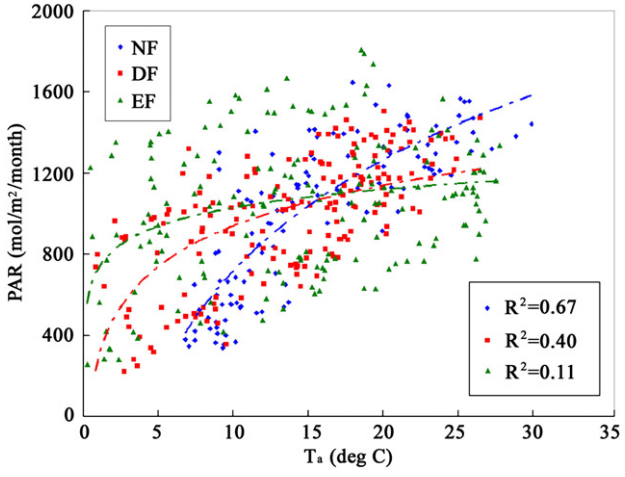

Fig. 4. Correlation between the air temperature (T_a) and the PAR for three plant functional types (NF, DF and EF represent non-forests, deciduous forests and evergreen forests, respectively).

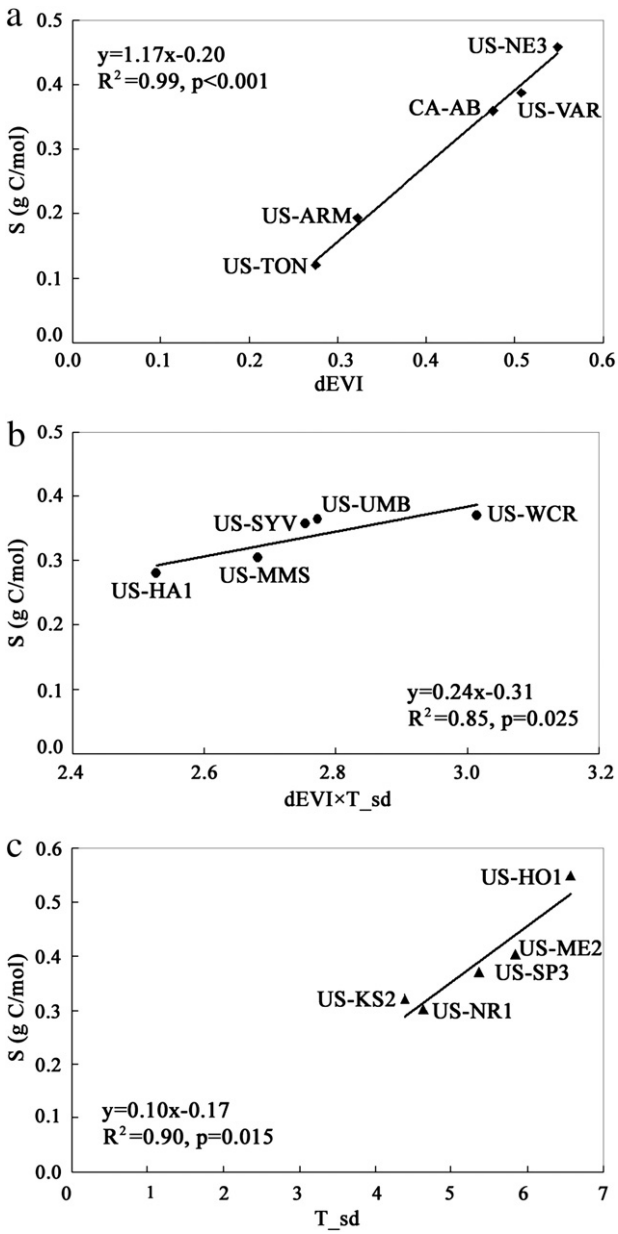

Fig. 5. Calibration of the GR model for sites of different plant functional types: a) NF sites, b) DF sites and c) EF sites, dEVI represents the difference between the maximum and minimum EVI and T_sd is the standard deviation of T_a.

may contribute little to photosynthesis because of the relatively low temperature (Chen et al., 2000). Furthermore, the chlorophyll content may increase faster than the biochemical capacity for carbon fixation during leaf development, which also leads to overestimation of GPP based on greenness. However, these leaves still increase the canopy greenness while flux measured GPP is not increasing. For EF sites, due to the low variations in greenness, this overestimation can be reduced to some extent. This is the reason for the disappearance of this overestimation for higher GPP values for all sites. The last reason is the improper characterizing of shaded leaves in the canopy for this type of models. This overestimation at low GPP may be associated with underestimation at high GPP because the slope from regression model only gives the mean conditions of the variables. To balance the underestimation at high GPP where shaded leaves contribute most, GPP is overestimated at low ranges. Similar results are observed in previous studies of Sims et al. (2008) and Peng et al. (2011), but reasons are not given. For example, the TG model which utilized the

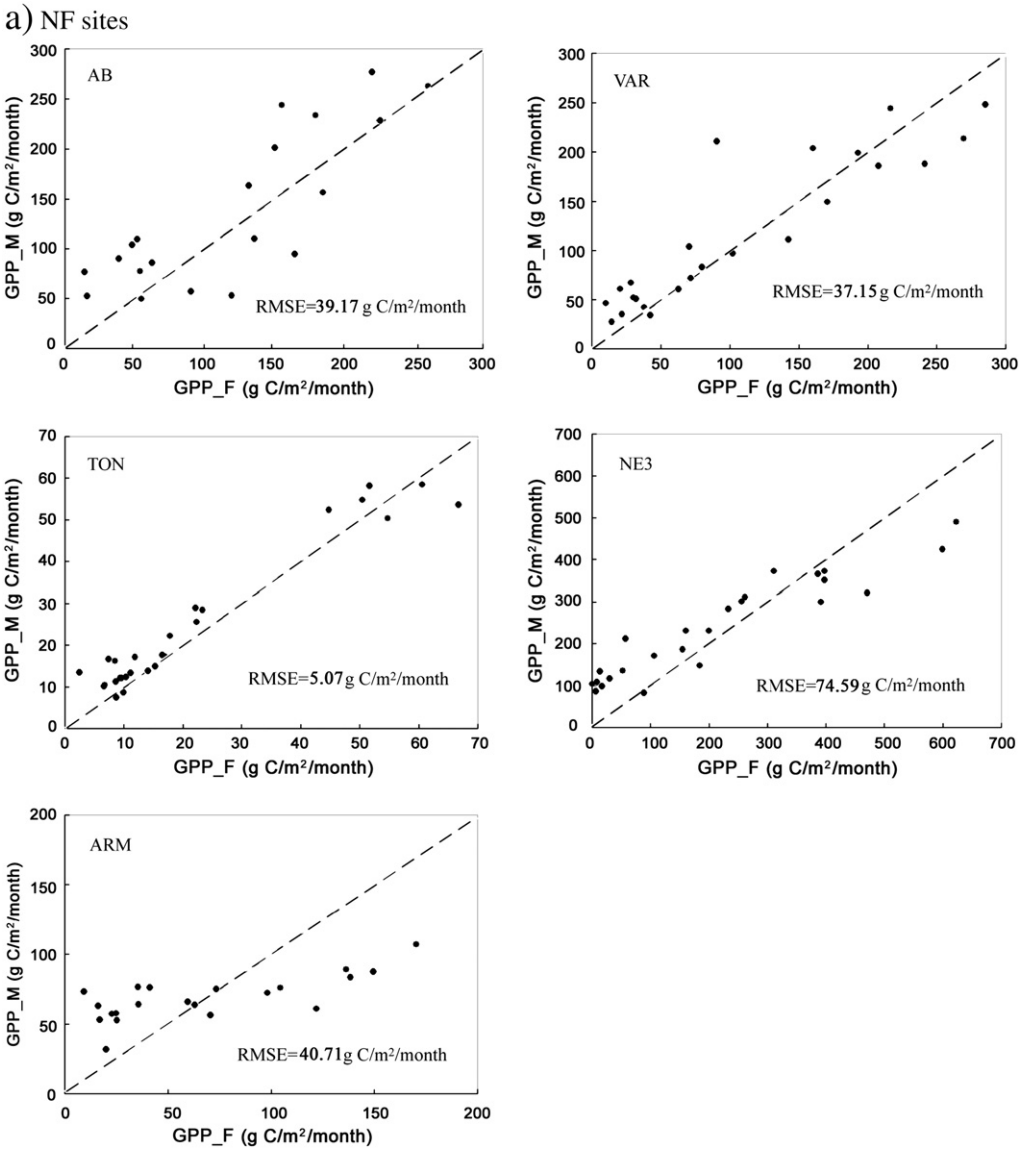

Fig. 6. Relationship between the flux measured GPP (GPP_F) and the calibrated GR model outputs (GPP_M) for each single site (the dash line indicates 1:1).

MODIS EVI shows overestimation of daily GPP at a value lower than 0.5 mol C/m^2/day (~180 g C/m^2/month) in DF sites while such discrepancy is not observed for low GPP values in EF sites. This typical limitation indicates that more emphasis should be focused on the ecophysiological considerations between vegetation and the environment as well as the incorporation of upscaling approaches from leaf to canopy level photosynthesis (Hilker et al., 2008, 2010; Mu et al., 2011; Zhao et al., 2006).

3.3. Discussion

The dependence of *S* on different variables for these three plant functional types shows the relative importance of aspects that affect the monthly GPP. Generally, monthly GPP is controlled by two sets of factors. First may be represented by the chlorophyll content within the canopy which is directly responsible for photosynthesis. This factor can be viewed as an "internal" impetus and can be quantified from remote sensing observations via a vegetation index. The second is the "external" factors such as water, temperature and radiation. These factors are often seen as stresses and show certain constraints on production. Here we suggest that the relative importance of these two drivers may vary in different plant functional types, which can be used to explain the different coefficients found in our model calibration.

In order to substantiate this suggestion, both T_a and EVI are selected to explore their usefulness in explaining the variances in monthly GPP for the three plant functional types (Fig. 8). For the NF sites, the constraint on vegetation production is largely dependent on the canopy greenness. This is validated with our data that an R^2 of 0.61 is obtained for GPP-EVI, which is much higher than that of GPP-T_a ($R^2 = 0.10$). This does not mean that the environmental variables (e.g., water, temperature) are not important because these factors can also affect the canopy greenness. Here we only argue that the dynamical range of greenness, for example, in terms of EVI, is the main control of the monthly GPP for the NF sites. This finding coincides with recent research which reports that slopes in the GPP model are related to the peak leaf area index (LAI) in the African ecosystems characterized by NF biomes (Sjöström et al., 2011).

However, for the EF sites with a relatively stable greenness indicated by low EVI_sd, variations in temperature may become a more important factor that determines the monthly production. This is because when canopy greenness is stable, other factors (e.g., temperature, soil) will play the limiting roles for vegetation production. For example, low correlation ($R^2 = 0.16$) between GPP and EVI is

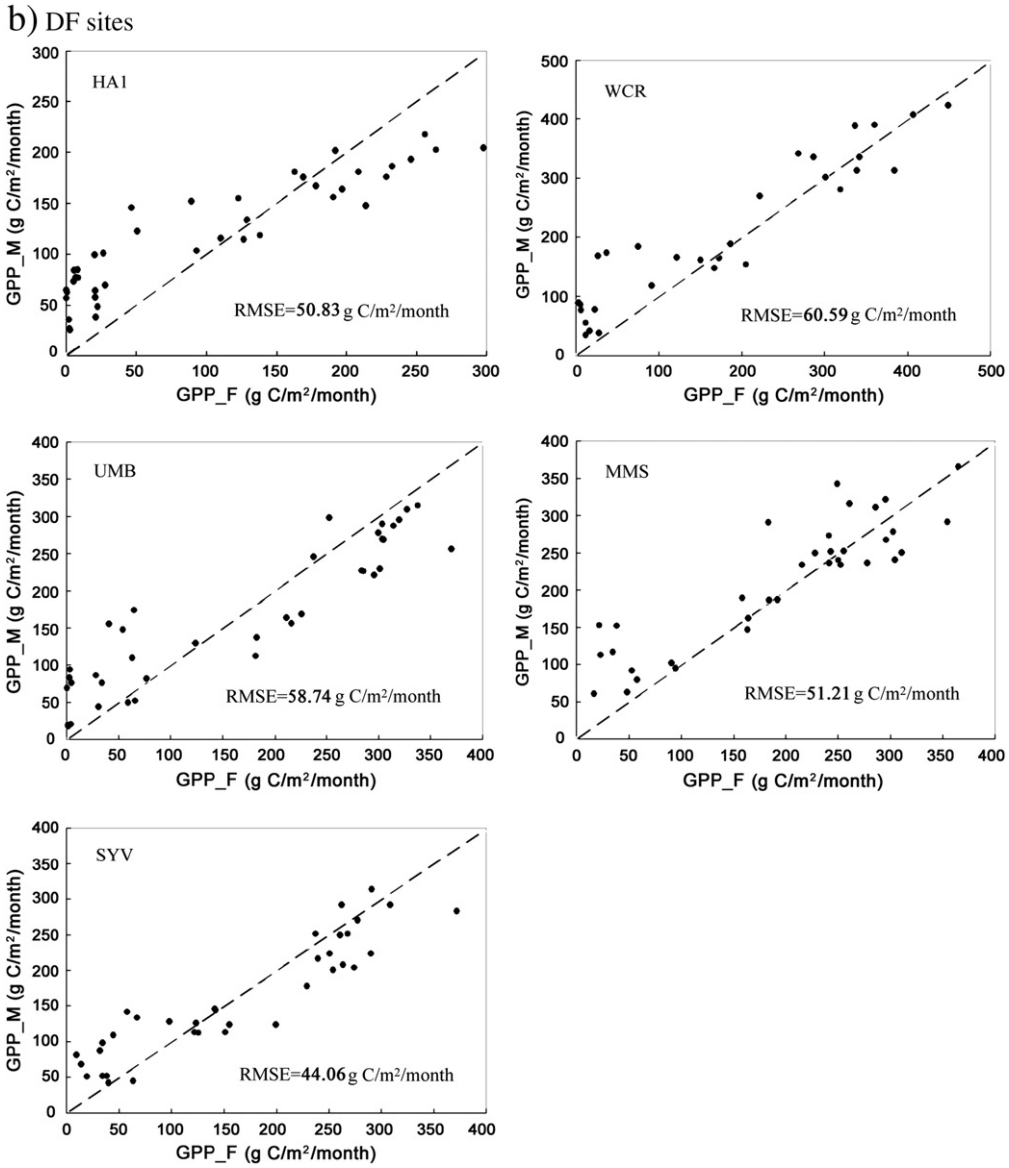

Fig. 6 (*continued*).

observed which means that the explained variance of GPP is very low while T_a can be a better indicator of GPP ($R^2 = 0.39$). The DF sites will fall between NF and EF species and therefore *S* is found to be a function of both canopy greenness and temperature variation. This analysis is consistent with the results shown in Fig. 8b, that R^2 values of 0.73 and 0.78 are found for GPP-T_a and GPP-EVI, respectively. The above analysis can be further supported by the correlation between *S* and EVI_sd for NF sites as well as the correlation between *S* and the difference in extreme values of temperature for EF sites (Fig. 9). Due to higher correlations shown in Fig. 4, these coefficients shown in Fig. 9 are not used for model calibration. However, similar implications are included in Figs. 4 and 9 which indicate that the different factors are in main control of monthly GPP for various plant function types. These results firstly demonstrate that model calibration across different biomes is a challenge since the relative importance of these various factors may change for different ecoregions. However, they may also lead to approaches to incorporate these potential variables in the GR model.

Another important potential of the GR model lies in its reduced dependence on input variables. For example, all the parameters could be directly acquired from remote sensing observations since MODIS already produces an EVI product. Remote estimation of PAR from MODIS aerosol type and atmospheric conditions will further make the GR model attractive for operational applications based on entirely remote sensing data (Liang et al., 2006). However, in these cases, the improved algorithms for cloud detection and removal are necessary for the use at global scale (Zhao et al., 2006). Nevertheless, evaluation of the GR model across biomes still gives the opportunity for its potential use in carbon cycle research and will be an important tool for the assessment of terrestrial ecosystem functions.

4. Conclusions

Terrestrial GPP is the largest carbon flux, and it drives several ecosystem functions, such as respiration and growth. Accurate estimation of this flux will be extremely useful for quantifying ecosystem carbon exchanges. Here we provide a multiple site evaluation of the GR model for estimating GPP in a range of ecosystems, representing diverse canopy structures and ecoregional characteristics. These results show that the GR model can provide good estimates of monthly

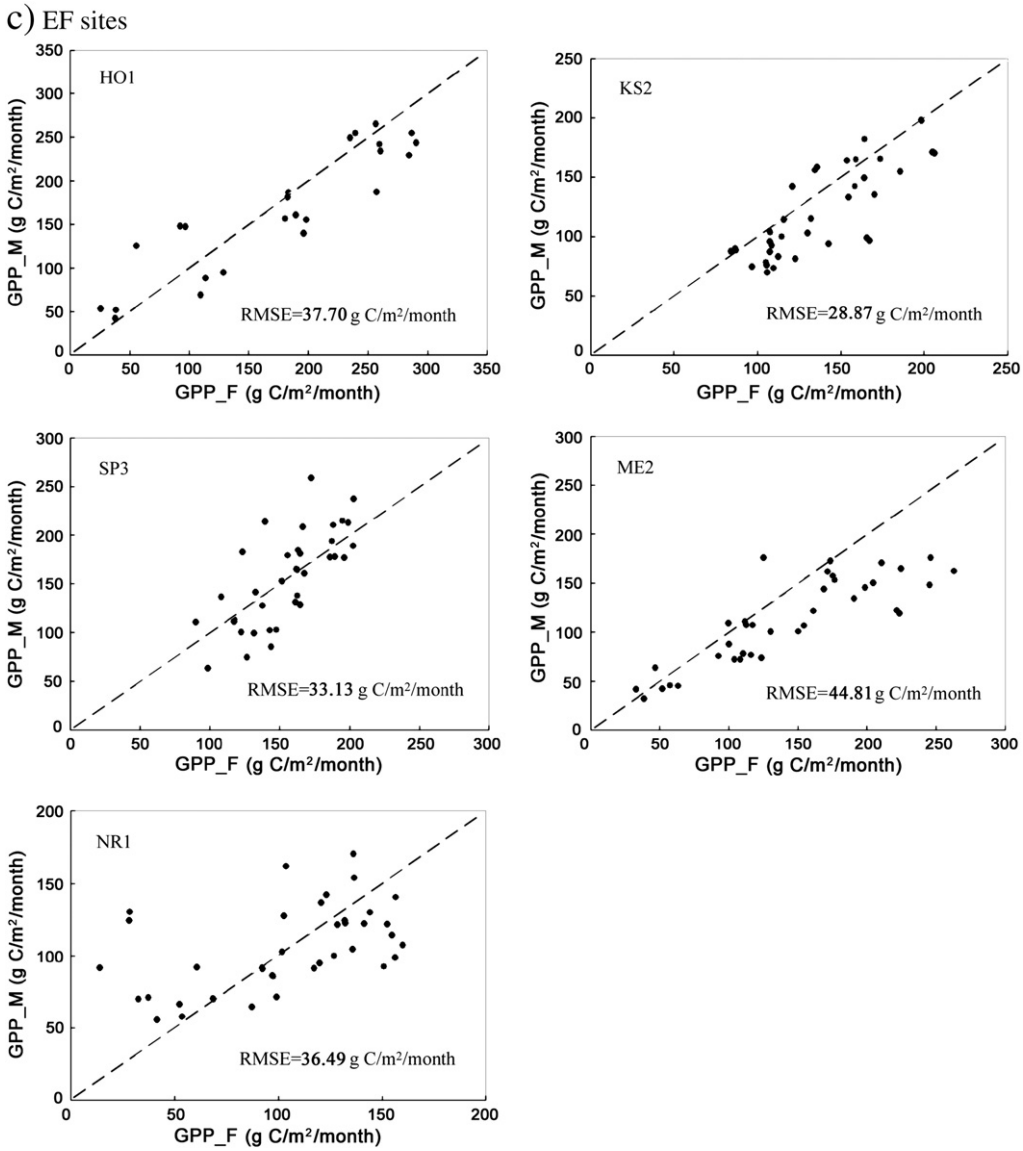

Fig. 6 (*continued*).

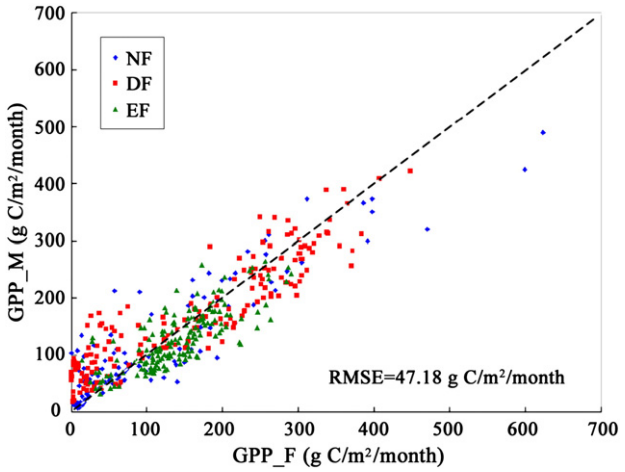

Fig. 7. Relationship between the flux measured GPP (GPP_F) and the calibrated GR model outputs (GPP_M) for the overall data (the dash line indicates 1:1). NF, DF and EF represent non-forests, deciduous forests and evergreen forests, respectively.

GPP for both NF and DF sites with moderate results for EF sites. Different dynamical ranges in the EVI and the relatively importance of various environmental factors may probably be the reasons for such differences. Nevertheless, the GR model can give a reasonably low RMSE of 47.18 g C/m^2/month for the overall dataset after model calibration, which indicates the potential of the model in future operational applications. A typical limitation of the GR model is the overestimation of GPP at the early growth seasons. This first indicates that the background signals for sparse vegetated areas may lead uncertainties to model application. However, this also gives the urgent needs of incorporation of such signals to improve the accuracy of model outputs. Future analysis may have a focus on the ecophysiological interactions between the ecosystem and the environmental variables.

Acknowledgement

We like to offer our thanks to Dr. Ankur R. Desai for his valuable suggestions and language editing. We also appreciate initial comments from Dr. David Y. Hollinger. This work used the data at the

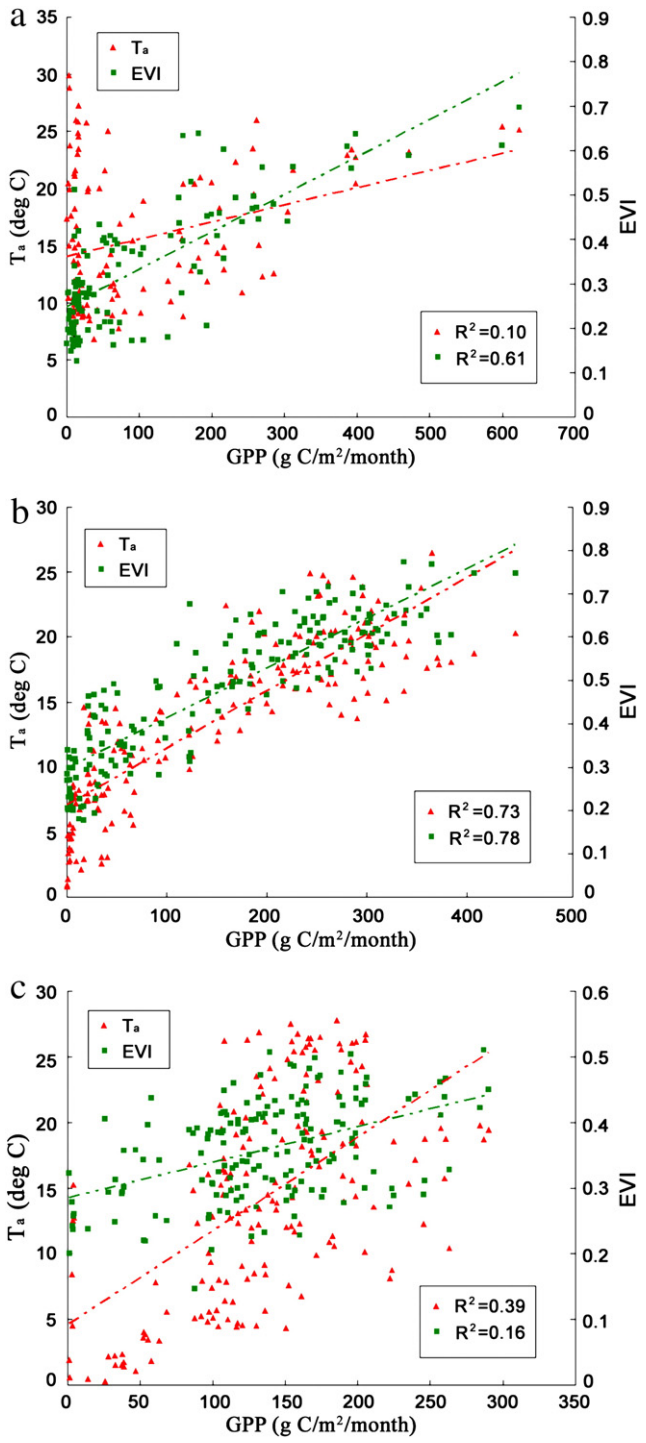

Fig. 8. Relationship between GPP and T_a, EVI for (a) Non-forests, (b) Deciduous forests and (c) Evergreen forests.

following sites from both the Ameriflux and Fluxnet-Canada: CA-AB, US-VAR, US-TON, US-NE3, US-ARM, US-HA1, US-UMB, US-MMS, US-WCR, US-SYV, US-NR1, US-HO1, US-ME2, US-SP3, US-KS2. We are grateful of PIs for the above sites in providing the data and explanations. This work was funded by an NSERC Strategic Grant (381474–09), the National Natural Science Foundation (Grant no. 41001210), the Knowledge Innovation Program of CAS (KZCX2-EW-QN302), and the Special Foundation for Young Scientists of IRSA (Y0S04800KB).

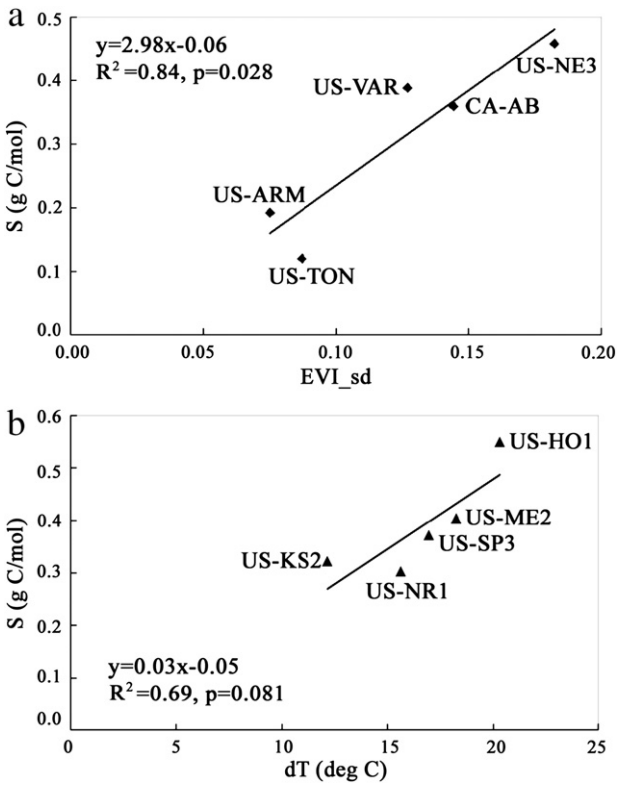

Fig. 9. The correlation between (a) the slope (S) and standard deviation in EVI (EVI_sd) in NF sites; (b) correlation between the slope (S) and difference in maximum and minimum temperature (dT) in EF sites.

References

Barr, A. G., Black, T. A., Hogg, E. H., Kljun, N., Morgenstern, K., & Nesic, Z. (2004). Interannual variability in the leaf area index of a boreal aspen-hazelnut forest in relation to net ecosystem production. *Agricultural and Forest Meteorology*, *126*, 237–255.

Beer, C., Reichstein, M., Tomelleri, E., Ciais, P., Jung, M., Carvalhais, N., et al. (2010). Terrestrial gross carbon dioxide uptake: Global distribution and covariation with climate. *Science*, *329*, 834–838.

Chen, W., Chen, J., Liu, J., & Cihlar, J. (2000). Approaches for reducing uncertainties in regional forest carbon balance. *Global Biogeochemical Cycles*, *14*, 827–838.

Cook, B. D., Davis, K. J., Wang, W., Desai, A., Berger, B. W., Teclaw, R. M., et al. (2004). Carbon exchange and venting anomalies in an upland deciduous forest in northern Wisconsin, USA. *Agricultural and Forest Meteorology*, *126*, 271–295.

Coops, N. C., Waring, R. H., & Law, B. E. (2005). Assessing the past and future distribution and productivity of ponderosa pine in the Pacific Northwest using a process model, 3-PG. *Ecological Modelling*, *183*, 107–124.

Curtis, P. S., Hanson, P. J., Bolstad, P., Barford, C., Randolph, J. C., Schmid, H. P., et al. (2002). Biometric and eddy-covariance based estimates of annual carbon storage in five eastern North American deciduous forests. *Agricultural and Forest Meteorology*, *113*, 3–19.

Desai, A. R., Noormets, A., Bolstad, P. V., Chen, J. Q., Cook, B. D., Davis, K. J., et al. (2008). Influence of vegetation and seasonal forcing on carbon dioxide fluxes across the Upper Midwest, USA: Implications for regional scaling. *Agricultural and Forest Meteorology*, *148*, 288–308.

Dore, S., Hymus, G. J., Johnson, D. P., Hinkle, C. R., Valentini, R., & Drake, B. G. (2003). Cross validation of open-top chamber and eddy covariance measurements of ecosystem CO_2 exchange in a Florida scrub-oak ecosystem. *Global Change Biology*, *9*, 84–95.

Dragoni, D., Schmid, H. P., Grimmond, C. S. B., & Loescher, H. W. (2007). Uncertainty of annual net ecosystem productivity estimated using eddy covariance flux measurements. *Journal of Geophysical Research*, *112*, D17102, doi:10.1029/2006JD008149

Fischer, M. L., Billesbach, D. P., Riley, W. J., Berry, J. A., & Torn, M. S. (2007). Spatiotemporal variations in growing season exchanges of CO_2, H_2O, and sensible heat in agricultural fields of the Southern Great Plains. *Earth Interactions*, *11*, 1–21.

Flanagan, L. B., & Johnson, B. G. (2005). Interacting effects of temperature, soil moisture and plant biomass production on ecosystem respiration in a northern temperate grassland. *Agricultural and Forest Meteorology*, *130*, 237–253.

Gitelson, A. A., Viña, A., Verma, S. B., Rundquist, D. C., Arkebauer, T. J., Keydan, G., et al. (2006). Relationship between gross primary production and chlorophyll content in crops: Implications for the synoptic monitoring of vegetation productivity. *Journal of Geophysical Research*, *111*, D08S11, doi:10.1029/2005JD006017

Goetz, S. J., Prince, S. D., & Small, J. (2000). Advances in satellite remote sensing of environmental variables for epidemiological applications. *Advances in Parasitology*, *47*, 289–307.

Hilker, T., Coops, N. C., Wulder, M. A., Black, T. A., & Guy, R. D. (2008). The use of remote sensing in light use efficiency based models of gross primary production: A review of current status and future requirements. *Science of the Total Environment*, *404*, 411–423.

Hilker, T., Hall, F. G., Coops, N. C., Lyapustin, A., Wang, Y., Nesic, Z., et al. (2010). Remote sensing of photosynthetic light-use efficiency across two forested biomes: Spatial scaling. *Remote Sensing of Environment*, *114*, 2863–2874.

Hollinger, D. Y., Aber, J., Dail, B., Davidson, E. A., Goltz, S. M., Hughes, H., et al. (2004). Spatial and temporal variability in forest-atmosphere CO_2 exchange. *Global Change Biology*, *10*, 1689–1706.

Huete, A., Didan, K., Miura, T., Rodriguez, E. P., Gao, X., & Ferreira, L. G. (2002). Overview of the radiometric and biophysical performance of the MODIS vegetation indices. *Remote Sensing of Environment*, *83*, 195–213.

Justice, C. O., Townshend, J. R. G., Vermote, E. F., Masuoka, E., Wolfe, R. E., Saleous, N., et al. (2002). An overview of MODIS Land data processing and product status. *Remote Sensing of Environment*, *83*, 3–15.

Liang, S., Zheng, T., Liu, R., Fang, H., Tsay, S. C., & Running, S. (2006). Estimation of incident photosynthetically active radiation from Moderate Resolution Imaging Spectrometer data. *Journal of Geophysical Research*, *111*, D15208, doi:10.1029/2005JD006730.

Ma, S. Y., Baldocchi, D. D., Xu, L. K., & Hehn, T. (2007). Inter-annual variability in carbon dioxide exchange of an oak/grass savanna and open grassland in California. *Agricultural and Forest Meteorology*, *147*, 157–171.

Monson, R. K., Sparks, J. P., Rosenstiel, T. N., Scott-Denton, L. E., Huxman, T. E., Harley, P. C., et al. (2005). Climatic influences on net ecosystem CO_2 exchange during the transition from wintertime carbon source to springtime carbon sink in a high-elevation, subalpine forest. *Oecologia*, *146*, 130–147.

Mu, Q., Zhao, M., & Running, S. W. (2011). Improvements to a MODIS global terrestrial evapotranspiration algorithm. *Remote Sensing of Environment*, *115*, 1781–1800.

Papale, D., & Valentini, A. (2003). A new assessment of European forests carbon exchange by eddy fluxes and artificial neural network spatialization. *Global Change Biology*, *9*, 525–535.

Peng, Y., Gitelson, A. A., Keydan, G. P., Rundquist, D. C., & Moses, W. J. (2011). Remote estimation of gross primary production in maize and support for a new paradigm based on total crop chlorophyll content. *Remote Sensing of Environment*, *115*, 978–989.

Powell, T. L., Gholz, H. L., Clark, K. L., Starr, G., Cropper, W. P., Jr., & Martin, T. A. (2008). Carbon exchange of a mature, naturally regenerated pine forest in north Florida. *Global Change Biology*, *14*, 2523–2538.

Reich, P. B. (2010). The carbon dioxide exchange. *Science*, *329*, 774–775.

Reichstein, M., Falge, E., Baldocchi, D., Papale, D., Aubinet, M., Berbigier, P., et al. (2005). On the separation of net ecosystem exchange into assimilation and ecosystem respiration: Review and improved algorithm. *Global Change Biology*, *11*, 1424–1439.

Ryu, Y., Baldocchi, D. D., Ma, S., & Hehn, T. (2008). Interannual variability of evapotranspiration and energy exchange over an annual grassland in California. *Journal of Geophysical Research*, *113*, D09104, doi:10.1029/2007JD009263.

Sims, D. A., Rahman, A. F., Cordova, V. D., El-Masri, B. Z., Baldocchi, D. D., Bolstad, P. V., et al. (2008). A new model of gross primary productivity for North American ecosystems based solely on the enhanced vegetation index and land surface temperature from MODIS. *Remote Sensing of Environment*, *112*, 1633–1646.

Sjöström, M., Ardö, J., Arneth, A., Boulain, N., Cappelaere, B., Eklundh, L., et al. (2011). Exploring the potential of MODIS EVI for modeling gross primary production across African ecosystems. *Remote Sensing of Environment*, *115*, 1081–1089.

Suyker, A. E., & Verma, S. B. (2008). Interannual water vapor and energy exchange in an irrigated maize-based agroecosystem. *Agricultural and Forest Meteorology*, *148*, 417–427.

Thomas, C. K., Law, B. E., Irvine, J., Martin, J. G., Pettijohn, J. C., & Davis, K. J. (2009). Seasonal hydrology explains inter-annual and seasonal variation in carbon and water exchange in a semi-arid mature Ponderosa Pine forest in Central Oregon. *Journal of Geophysical Research*, *114*, G04006, doi:10.1029/2009JG001010.

Urbanski, S., Barford, C., Wofsy, S., Kucharik, C., Pyle, E., Budney, J., et al. (2007). Factors controlling CO_2 exchange on timescales from hourly to decadal at Harvard Forest. *Journal of Geophysical Research*, *112*, G02020, doi:10.1029/2006JG000293.

Wan, Z. (2008). New refinements and validation of the MODIS Land-Surface Temperature/Emissivity products. *Remote Sensing of Environment*, *112*, 59–74.

Westermann, S., Langer, M., & Boike, J. (2011). Spatial and temporal variations of summer surface temperatures of high-arctic tundra on Svalbard-Implications for MODIS LST based permafrost monitoring. *Remote Sensing of Environment*, *115*, 908–922.

Wu, C., Munger, J. W., Niu, Z., & Kuang, D. (2010). Comparison of multiple models for estimating gross primary production using MODIS and eddy covariance data in Harvard Forest. *Remote Sensing of Environment*, *114*, 2925–2939.

Wu, C., Niu, Z., Tang, Q., Huang, W., Rivard, B., & Feng, J. (2009). Remote estimation of gross primary production in wheat using chlorophyll-related vegetation indices. *Agricultural and Forest Meteorology*, *149*, 1015–1021.

Xiao, X., Zhang, Q., Braswell, B., Urbanski, S., Boles, S., Wofsy, S., et al. (2004). Modeling gross primary production of temperate deciduous broadleaf forest using satellite images and climate data. *Remote Sensing of Environment*, *91*, 256–270.

Zhao, M., & Running, S. W. (2010). Drought-induced reduction in global terrestrial net primary production from 2000 through 2009. *Science*, *329*, 940–943.

Zhao, M., Running, S. W., & Nemani, R. R. (2006). Sensitivity of Moderate Resolution Imaging Spectroradiometer (MODIS) terrestrial primary production to the accuracy of meteorological reanalyses. *Journal of Geophysical Research*, *111*, G01002, doi:10.1029/2004JG000004.